Inorg. Chem. **2008**, *47*, 7190−7201

Highly Sensitive Multiresponsive Chemosensor for Selective Detection of Hg^{2+} in Natural Water and Different Monitoring Environments

Dayu Wu,[†] Wei Huang,[†] Zhihua Lin,[‡] Chunying Duan,*[,‡] Cheng He,[‡] Shuo Wu,[‡] and Dehui Wang[‡]

State Key Laboratory of Coordination Chemistry, Nanjing University, Nanjing 210093, China, and State Key Laboratory of Fine Chemicals, Dalian University of Technology, Dalian 116012, China

Received March 10, 2008

A new chemosensor **RF1** that combines a ferrocene unit and a rhodamine block via the linkage of a carbohydrazone binding unit was designed and prepared for the highly selective detection of Hg^{2+} in natural water. This chemosensor displays great brightness and fluorescence enhancement following Hg^{2+} coordination within the limit of detection for Hg^{2+} at 1 parts per billion (ppb). The fluorescence intensities are nearly proportional to the amount of Hg^{2+} at the ppb level. It is capable of distinguishing between the safe and the toxic levels of inorganic mercury in drinking water. Hg^{2+}-binding also arouses the absorption of the rhodamine moiety in **RF1** significantly with the chromogenic detection limit for Hg^{2+} at 50 ppb. The conventional UV-vis spectroscopic method thus has the potential to provide the critical information about the mercury hazard assessment for industrial wastewater discharging. The obvious and characteristic color change of the titration solution from colorless to pink upon the addition of Hg^{2+} demonstrates that **RF1** can be used for "naked-eye" detection of Hg^{2+} in water. The Hg^{2+} complexation also causes a significant shift of the redox potential about the ferrocene/ferrocenium couple. The electrochemical responses provide the possibility to quantitative analysis of Hg^{2+} at the parts per million (ppm) level. Preliminary investigations in natural water samples including seawater and freshwater indicate that **RF1** offers a direct and immediate Hg^{2+} detection in complex media, pointing out its potential utility in environment monitoring and assessment. The responses of **RF1** are Hg^{2+} specific, and the chemosensor exhibits high selectivity toward Hg^{2+} over other Group 12 metals, alkali, alkaline earth metals, and most of the divalent first-row transition metals. The **RF1**-Hg^{2+} complex is successfully isolated and the Hg^{2+}-binding is reversible. The crystal structure and spectral properties of its congener **RF2** that contains one ferrocene group and two rhodamine 6G moieties were also investigated for a comparison.

Introduction

Mercury is a widespread pollutant with distinct toxicological profiles. Despite a reduction of its industrial use as a result of stricter regulations, high concentrations of mercury are still present in many environmental compartments. It is found in many products of daily life such as paints, electronic equipment, and batteries,[1–3] and it exists in a variety of different forms (metallic, ionic, and as part of organic and inorganic salts and complexes).[4–6] These environmental and health problems have prompted the development of methods for the detection and quantification of mercury applicability, especially in situations where conventional techniques are not appropriate. So far, significant progress in the creation of the highly sensitive redox,[7,8] chromogenic,[9–11] or fluorogenic[12–21] probes has been achieved. A promising way is to synthesize a molecule that is capable of reporting on the recognition of Hg^{2+} through a variety of physical responses, which allows the same sensor to be applied in various experimental conditions.[22–24]

* To whom correspondence should be addressed. E-mail: cyduan@dlut.edu.cn.
[†] State Key Laboratory of Coordination Chemistry, Nanjing University.
[‡] State Key Laboratory of Fine Chemicals, Dalian University of Technology.

(1) Clarkson, T. W.; Magos, L.; Myers, G. J. *N. Engl. J. Med.* **2003**, *349*, 1731–1737.
(2) Davidson, P. W.; Myers, G. J.; Cox, C.; Axtell, C.; Shamlaye, C.; Sloane-Reeves, J.; Cernichiari, E.; Needham, L.; Choi, A.; Wang, Y.; Berlin, M.; Clarkson, T. W. *J. Am. Med. Assoc.* **1998**, *280*, 701–707.
(3) Wang, Q. R.; Kim, D.; Dionysiou, D. D.; Sorial, G. A.; Timberlake, D. *Environ. Pollut.* **2004**, *131*, 323–336.
(4) Renzoni, A.; Zino, F.; Franchi, E. *Environ. Res., Sect. A* **1998**, *77*, 68–72.
(5) Bolger, P. M.; Schwetz, B. A. *N. Engl. J. Med.* **2002**, *347*, 1735–1736.
(6) Harris, H. H.; Pickering, I. J.; George, G. N. *Science* **2003**, *301*, 1203.

10.1021/ic8004344 CCC: $40.75
Published on Web 07/19/2008

Because the fluorometric methods can reach a much lower detection limit and the instrumentation involved is widely available, Hg^{2+}-responsive chemosensors with fluorescence response offer a promisingly simple and rapid approach in monitoring the aqueous Hg^{2+} in biological and environmental samples. An important practical challenge to achieve this goal is to obtain water-soluble fluorescent dyes, which can meet the criteria of appropriate selectivity over the competing metal ion contaminants and of optical sensitivity in aqueous solution.[25–33] In particular, one common limitation for heavy-metal detection in the environment is the low quantum efficiency of metal bound dyes in water compared to that in organic or in mixed aqueous−organic solvents. In addition, on the basis of the maximum level (2 parts per billion (ppb)) of mercury in drinking water permitted by the United States Environmental Protection Agency (EPA),[34] an ideal probe should display a very low detection limit and retain its selectivity toward Hg^{2+} in the presence of other metals with higher concentrations.[35–37]

In the mean time, the in situ mercury-indicating methodologies for rapid screening applications have the potential to provide critical information about the mercury hazard assessment and mercury pollution management for the industrial wastewater. In this case, the easy-accessed "naked eye" colorimetric probes[38,39] and electrochemical sensing devices[40,41] that can detect the concentrations of mercury in real-time play a leading role, particular in utilizing molecular probes to generate and transduce an analytical signal as a response to the binding event. However, the present chromophoric probes are either limited with respect to their low sensitivity and selectivity or incompatible with aqueous environments,[42,43] and only a few of them can be used as practical probes for in situ quantitative Hg^{2+} analysis in aqueous media.[44,45]

Because of the large molar extinction coefficient (ε) and the high fluorescence quantum yield (Φ), rhodamine-based dyes have been used as effective dual responsive optical probes via chromogenical and fluorogenical signals.[46–48] On the other hand, ferrocene-based receptors usually exhibit a significant potential shift of the Fe^{III}/Fe^{II} redox couple on complexation of an analyte[49–51] and have been involved in a multiresponsive signaling event.[52–55] By combining a ferrocene unit with a rhodamine-6G block into one molecule via a carbohydrazone linkage, we try to develop a new and practical multiresponsive chemosensor (Scheme 1) for the detection of Hg^{2+} in aqueous media. It is expected that the introduction of an electron-rich ferrocenyl group could enhance the coordination ability of the hydrazone nitrogen atom to Hg^{2+} ion,[56] and high sensitivity for Hg^{2+} would be realized in neutral water with the detection limit down to

(7) Lloris, J. M.; Martínez-Máñez, R.; Padilla-Tosta, M. E.; Pardo, T.; Soto, J.; Beer, P. D.; Cadman, J.; Smith, D. K. *J. Chem. Soc., Dalton Trans.* **1999**, 2359–2369.
(8) Nolan, M. A.; Kounaves, S. P. *Anal. Chem.* **1999**, *71*, 3567–3573.
(9) Ros-Lis, J. V.; Martínez-Máñez, R.; Rurack, K.; Sancenon, F.; Soto, J.; Spieles, M. *Inorg. Chem.* **2004**, *43*, 5183–5185.
(10) Huang, J. H.; Wen, W. H.; Sun, Y. Y.; Chou, P. T.; Fang, J. M. *J. Org. Chem.* **2005**, *70*, 5827–5832.
(11) Tatay, S.; Gavina, P.; Coronado, E.; Palomares, E. *Org. Lett.* **2006**, *8*, 3857–3860.
(12) Kim, I. B.; Bunz, U. H. F. *J. Am. Chem. Soc.* **2006**, *128*, 2818–2819.
(13) Zhao, Y.; Zhong, Z. *J. Am. Chem. Soc.* **2006**, *128*, 9988–9989.
(14) Cheng, P.; He, C. *J. Am. Chem. Soc.* **2004**, *126*, 728–729.
(15) Métivier, R.; Leray, I.; Valeur, B. *Chem.−Eur. J.* **2004**, *10*, 4480–4490.
(16) Dickerson, T. J.; Reed, N. N.; LaClair, J. J.; Janda, K. D. *J. Am. Chem. Soc.* **2004**, *126*, 16582–16586.
(17) Zhang, G.; Zhang, D.; Yin, S.; Yang, X.; Shuai, Z.; Zhu, D. *Chem. Commun.* **2005**, 2161–2163.
(18) Liu, B.; Tian, H. *Chem. Commun.* **2005**, 3156–2158.
(19) Ros-Lis, J. V.; Marcos, M. D.; Martínez-Máñez, R.; Rurack, K.; Soto, J. *Angew. Chem., Int. Ed.* **2005**, *44*, 4405–4407.
(20) Kim, S. H.; Kim, J. S.; Park, S. M.; Chang, S. K. *Org. Lett.* **2006**, *8*, 371–374.
(21) Song, K. C.; Kim, J. S.; Park, S. M.; Chung, K. C.; Ahn, S.; Chang, S. K. *Org. Lett.* **2006**, *8*, 3413–3416.
(22) Caballero, A.; Martínez-Máñez, R.; Lloveras, V.; Ratera, I.; Vidal-Gancedo, J.; Wurst, K.; Tarraga, A.; Molina, P.; Veciana, J. *J. Am. Chem. Soc.* **2005**, *127*, 15666–15667.
(23) Nazeeruddin, M. K.; Di Censo, D.; Humphry-Baker, R.; Grätzel, M. *Adv. Funct. Mater.* **2006**, *16*, 9–194.
(24) Zhao, Q.; Cao, T. Y.; Li, F. Y.; Li, X. H.; Jing, H.; Yi, T.; Huang, C. H. *Organometallics* **2007**, *26*, 2077–2081.
(25) Nolan, E. M.; Lippard, S. T. *J. Am. Chem. Soc.* **2007**, *129*, 5910–5918.
(26) Ko, S. K.; Yang, Y. K.; Tae, J.; Shin, I. *J. Am. Chem. Soc.* **2006**, *128*, 14150–14155.
(27) Zhao, Y.; Zhong, Z. *Org. Lett.* **2006**, *8*, 4715–4717.
(28) Wang, J.; Qian, X. *Org. Lett.* **2006**, *8*, 3721–3724.
(29) Ono, A.; Togashi, H. *Angew. Chem., Int. Ed.* **2004**, *43*, 4300–4302.
(30) Ou, S. J.; Lin, Z. H.; Duan, C. Y.; Zhang, H.; Bai, Z. P. *Chem. Commun.* **2006**, 4392–4394.
(31) Guo, X. F.; Qian, X. H.; Jia, L. H. *J. Am. Chem. Soc.* **2004**, *126*, 2272–2273.
(32) Yoon, S.; Miller, E. W.; He, Q.; Do, P. J.; Chang, C. J. *Angew. Chem., Int. Ed.* **2007**, *46*, 6658–6661.
(33) Huang, C. C.; Yang, Z.; Lee, K. H.; Chang, H. T. *Angew. Chem., Int. Ed.* **2007**, *46*, 6824–6828.
(34) *Mercury Update: Impact on Fish Advisories*; EPA Fact Sheet EPA-823-F-01−011; EPA, Office of Water: Washington, DC, 2001.
(35) Nolan, E. M.; Racine, M. E.; Lippard, S. J. *Inorg. Chem.* **2006**, *45*, 2742–2749.
(36) Nolan, E. M.; Lippard, S. J. *J. Am. Chem. Soc.* **2003**, *125*, 14270–14271.
(37) Descalzo, A. B.; Martínez Máñez, R.; Radeglia, R.; Rurack, K.; Sato, J. *J. Am. Chem. Soc.* **2003**, *125*, 3418–3419.
(38) Zhang, X. B.; Guo, C. C.; Li, Z. Z.; Shen, G. L.; Yu, R. Q. *Anal. Chem.* **2002**, *74*, 821–825.
(39) Safavi, A.; Bagheri, M. *Sens. Actuators, B* **2004**, *99*, 608–612.
(40) Tchinda, A. J.; Ngameni, E.; Walcarius, A. *Sens. Actuators, B* **2007**, *121*, 113–123.
(41) Singh, P. R.; Contractor, A. Q. *Int. J. Environ. Anal. Chem.* **2005**, *85*, 831–835.
(42) Ho, I. T.; Lee, G. H.; Chung, W. S. *J. Org. Chem.* **2007**, *72*, 2434–2442.
(43) Lee, M. H.; Cho, B. K.; Yoon, J. Y.; Kim, J. S. *Org. Lett.* **2007**, *9*, 4515–4518.
(44) Lee, J. S.; Han, M. S.; Mirken, C. A. *Angew. Chem., Int. Ed.* **2007**, *46*, 4093–4096.
(45) Coronado, E.; Galan-Mascaros, J. R.; Marti-Gastaldo, G.; Palomares, E.; Durrant, J. R.; Vilar, R.; Gratzel, M.; Nazeernddin, M. K. *J. Am. Chem. Soc.* **2005**, *127*, 12351–12356.
(46) Huang, C. C.; Chang, H. T. *Anal. Chem.* **2006**, *78*, 8332–8338.
(47) Yang, Y. K.; Yook, K. J.; Tae, J. *J. Am. Chem. Soc.* **2005**, *127*, 16760–16761.
(48) Ko, S. K.; Yang, Y. K.; Tae, J. S.; Shin, I. J. *J. Am. Chem. Soc.* **2006**, *128*, 14150–14155.
(49) Beer, P. D. *Acc. Chem. Res.* **1998**, *31*, 71–80.
(50) Ornelas, C.; Aranzaes, J. R.; Cloutet, E.; Alves, S.; Astruc, D. *Angew. Chem., Int. Ed.* **2007**, *46*, 872–877.
(51) Otón, F.; Tárraga, A.; Espinosa, A.; Velasco, M. D.; Molina, P. *Dalton Trans.* **2006**, 3685–3692.
(52) Lopez, J. L.; Tarraga, A.; Espinosa, A.; Velasco, M. D.; Molina, P.; Lloveras, V.; Vidal-Gancedo, J.; Rovira, C.; Veciana, J.; Evans, D. J.; Wurst, K. *Chem.−Eur. J.* **2004**, *10*, 1815–1826.
(53) Otón, F.; Tárraga, A.; Tarraga, A.; De Arellano, C. R.; Molina, P. *Chem.−Eur. J.* **2007**, *13*, 5742–5752.
(54) Zapata, F.; Caballero, A.; Espinosa, A.; Tarraga, A.; Molina, P. *Org. Lett.* **2007**, *9*, 2385–2388.
(55) Delavaux-Nicot, B.; Maynadié, J.; Lavabre, D.; Fery-Forgues, S. *Inorg. Chem.* **2006**, *45*, 5691–5702.

Scheme 1. Syntheses of **RF1** and **RF2**

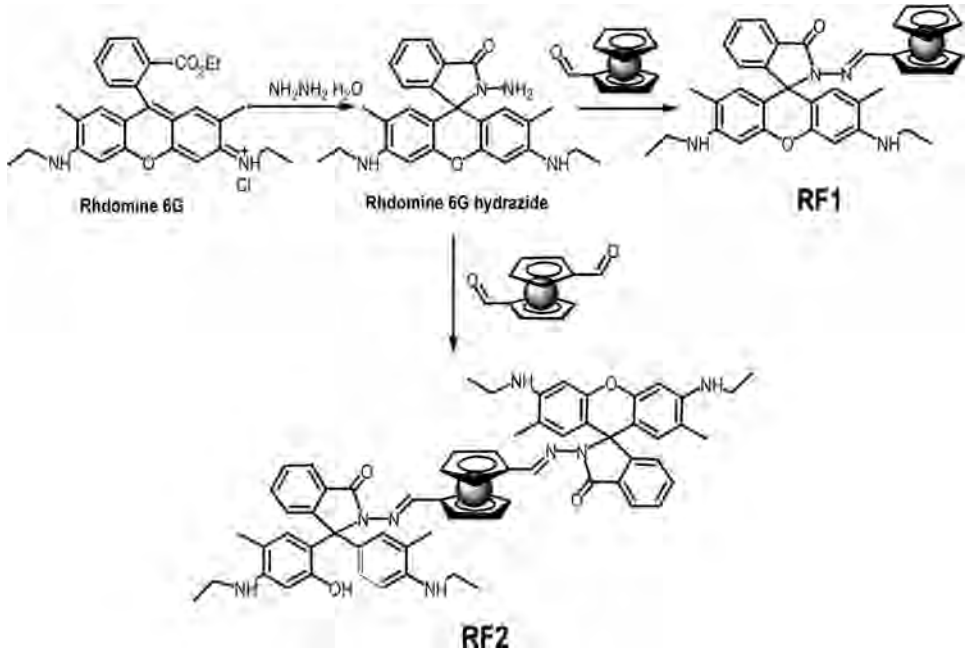

the ppb level. Meanwhile, the spatial effects of the uncoordinated ferrocenyl group are likely to affect the coordination ability of **RFs** to the transition metal ions with constraint geometries and certain coordination numbers. This would thus improve the selectivity of **RFs** for detecting Hg^{2+} over transition metal ions, a crucial issue for the practical application.

Experimental Section

Materials. All the chemicals were of analytic grade and used as received. Water used was redistilled. ^{1}H NMR and ^{13}C NMR spectra were recorded on a VARIAN INOVA-400 spectrometer with chemical shifts reported as parts per million (ppm; in DMSO-d_6, TMS as internal standard). Mass spectrometric data were obtained on a HP1100LC/MSD mass spectrometer and a LCQ-Tof MS spectrometer. Fluorescence spectra were determined on AB-series 2 and FS920 luminescence spectrometer (Edinburgh Instruments). Absorption spectra were measured on a Lambda 35 UV/vis spectrophotometer. All pH measurements were made with a Model PHS-3C meter. Elemental analyses (C, H, and N) were carried out on a Perkin-Elmer 240 analyzer. Rhodamine-6G hydrazide is prepared according to the literature method.[57] Cyclic voltammetric experiments were performed under nitrogen gas in CH_3CN or CH_3CN/H_2O (7:3) at a scan rate of 100 mV s^{-1} on a CHI 660B potentiostatic instrument at room temperature. The three-electrode cell comprises a 1 mm platinum-disk working electrode, a platinum-wire auxiliary electrode, and an SCE reference electrode. The electrolyte is n-Bu_4NClO_4 (0.1 mol dm^{-3}). Differential pulse voltammetry (DPV) measurements were also carried out using a CHI 660B with a 50 ms pulse width. The test paper was prepared by soaking the common filter paper (size 3 × 0.5 cm) in DMF solution of **RF1** (1 mM) at room temperature overnight and then dried in the dark in air.

RF1. Rhodamine 6G hydrazide (1.0 mmol, 0.43 g) and ferrocenecarboxaldehyde (1.0 mmol, 0.21 g) were mixed in a methanol solution with 0.1 mL of glacial acetic acid. After refluxing for 2 h, red precipitates obtained were filtered off, washed with methanol/ether (1:1) and dried over P_2O_5 under vacuum. Crystals suitable for X-ray structural analysis were obtained by carefully evaporating a methanol/acetontrile (1:1) solution in air. Yield: 0.55 g (88%). Anal. Calcd for **RF1**, $C_{37}H_{36}N_4O_2Fe$: H, 5.81; C, 71.13; N, 8.97. Found: H, 5.83; C, 71.22; N, 8.98. ESI-MS: m/z 625.4 for [**RF1** + H]$^+$. ^{1}H NMR (DMSO-d_6) δ(ppm): 8.088 (1 H, s, *CH*=*N*), 7.861 (1 H, d, J = 7.2 Hz, *Rh*-H), 7.535 (2 H, t, J = 6.8 Hz, *Rh*-H), 6.976 (1 H, d, J = 7.6 Hz, *Rh*-H), 6.367 (2 H, s, *Rh*-H), 6.206 (2 H, s, *Rh*-H), 5.087 (2H, s, *NH*), 4.355 (2 H, s, *Cp*-H), 4.305 (2 H, s, *Cp*-H), 3.827 (5 H, s, *Cp*-H), 3.145 (4H, m, J = 6.8 Hz, CH_2), 1.851 (6 H, s, CH_3), 1.190 (6 H, t, J = 6.8 Hz, CH_3).

RF2. Rhodamine 6G hydrazide (2.0 mmol, 0.86 g) and 1,1′-ferrocenedicarboxaldehyde (1.0 mmol, 0.24 g) were mixed in a methanol solution with three drops of acetic acid. After refluxing for 4 h, orange precipitates obtained were filtered off, washed with methanol/ether (1:1), and dried over P_2O_5 under vacuum. Crystals suitable for X-ray structural analysis were obtained by carefully evaporating a dichloromethane solution in air. Yield: 0.95 g (77%). Anal. Calcd for **RF2**, $C_{66}H_{66}Cl_4FeN_8O_4$: H, 5.41; C, 64.37; N, 9.11. Found: H, 5.31; C, 64.23; N, 9.03. ^{1}H NMR (DMSO-d_6) δ(ppm): 8.018 (2 H, *d*, J = 4.8 Hz, *Rh*-H), 7.880 (2 H, *s*, *CH*=*N*), 7.454 (4 H, *t*, J = 4.4 Hz *Rh*-H), 7.034 (2 H, *d*, J = 4.4 Hz), 6.504 (4 H, s, *Rh*-H), 6.376 (4 H, s, *Rh*-H), 5.300 (4 H, *s*, *NH*), 4.059 (4H, s, *Cp*-H), 3.668 (4 H, s, *Cp*-H), 3.159 (8 H, q, J = 6.8 Hz, CH_2), 1.868 (12 H, s, CH_3), 1.235 (12 H, t, J = 6.8 Hz, -CH_3).

RF1-Hg. $Hg(NO_3)_2 \cdot 0.5H_2O$ (0.10 mmol, 0.033 g) dissolved in 15 mL of methanol/acetonitrile (8:2, v/v) was added to a suspension of **RF1** (0.1 mmol, 0.063 g) in 10 mL of methanol. The solution was refluxed for 20 min to obtain a clear red solution. Red powder obtained after slowly evaporating the solution in air was filtered off, washed with methanol/ether (1:1), and dried over P_2O_5 under vacuum. Yield: 0.075 g, (79%, based on **RF1**). Anal. Calcd for $C_{37}H_{36}FeN_4O_2Hg \cdot 2NO_3$: H, 3.82; C, 46.73; N, 8.84. Found: H, 4.12; C, 46.81; N, 8.75. ESI-MS: m/z = 888.18 for [Hg-

(56) González-Rodríguez, D.; Torres, T.; Olmstead, M. M.; Rivera, J.; Herranz, M. A.; Echegoyen, L.; Castellanos, C. A.; Guldi, D. M. *J. Am. Chem. Soc.* **2006**, *128*, 10680–10681.
(57) Yang, X. F.; Guo, X. Q.; Zhao, Y. B. *Talanta* **2002**, *57*, 883–890.

RF1$(NO_3)]^+$. ^{1}H NMR (DMSO-d_6) δ(ppm): 8.043 (1 H, s, *CH*=*N*), 7.860 (1 H, d, $J = 7.2$ Hz, *Rh*-H), 7.536 (2 H, t, $J = 6.8$ Hz, *Rh*-H), 6.972 (1 H, d, $J = 7.2$ Hz, *Rh*-H), 6.368 (2 H, s, *Rh*-H), 6.194 (2 H, s, *Rh*-H), 4.350 (2 H, s, *Cp*-H), 4.304 (2 H, s, *Cp*-H), 3.813 (5 H, s, *Cp*-H), 3.131 (4 H, m, $J = 6.8$ Hz, CH_2), 1.840 (6 H, s, CH_3), 1.174 (6 H, t, $J = 6.8$ Hz, CH_3).

Crystallography. Intensities of compounds **RF1** and **RF2** were collected on a Siemens SMART-CCD diffractometer with graphite-monochromated Mo Kα ($\lambda = 0.71073$ Å) using the SMART and SAINT programs.[58] Crystallographic data for **RF1**: $C_{37}H_{36}FeN_4O_2$, $M_r = 624.55$, monoclinic, $P2_1/c$, $a = 8.612(9)$ Å, $b = 22.42(2)$ Å, $c = 21.65(2)$ Å, $\beta = 100.72(1)°$, $V = 3005(2)$ Å^3, $Z = 4$, $D_{calcd} = 1.380$ g cm^{-3}, $T = 293(2)$ K. The final refinement gave $R_1 = 0.0562$, $wR_2 = 0.0755$ and GoF = 1.023 for 3032 observed reflections with $I > 2\sigma(I)$. Crystallographic data for **RF2**: $C_{66}H_{66}Cl_4FeN_8O_4$, $M_r = 1232.92$, monoclinic, $C2/c$, $a = 34.780(3)$ Å, $b = 9.508(1)$ Å, $c = 19.390(2)$ Å, $\beta = 109.801(4)°$, $V = 6033(2)$ Å^3, $Z = 4$, $D_{calcd} = 1.357$ g cm^{-3}, $T = 293(2)$ K. The final refinement gave $R_1 = 0.0556$, $wR_2 = 0.1601$ and GoF = 1.024 for 3315 observed reflections with $I > 2\sigma(I)$. The structures were resolved by direct methods and refined on F^2 by full-matrix least-squares methods with SHELXTL version 5.1.[59] Non-hydrogen atoms were refined anisotropically except the disordered solvent molecules. Hydrogen atoms were fixed geometrically at calculated distances and allowed to ride on the parent non-hydrogen atoms with the isotropic displacement being fixed at 1.2 and 1.5 times of the aromatic and methyl carbon atoms attached, respectively. For compound **RF1**, the acetonitrile molecules were disordered into two parts with the site occupancy factors of the atoms fixed at 0.5.

Preparation of Fluorometric Metal Ion Titration Solutions. Fluorescence titration spectra were obtained using the FS920 spectrometer (Edinburgh Instruments). Selectivity experiments were checked with an AB series2 luminescence spectrometer. Stock solution (2×10^{-2} M) of the aqueous perchlorate salts of K^+, Na^+, Ca^{2+}, Mg^{2+}, Co^{2+}, Ni^{2+}, Cu^{2+}, Mn^{2+}, Zn^{2+}, Cd^{2+}, Fe^{2+}, Ag^+, Pb^{2+}, and Hg^{2+} were prepared. High concentration of the stock solutions of **RF1** (1.0×10^{-3} M) were prepared in N,N′-dimethylformamide or acetonitrile, respectively. Before spectroscopic measurements, the solution of **RF1** (1 μM, or 0.1 μM) was freshly prepared by diluting the high concentration stock solution using a neutral aqueous solution. The fluorescence quantum yield was determined using optically matching solutions of rhodamine-6G ($\Phi_f = 0.94$ in ethanol) as standard at an excitation wavelength of 500 nm, and the quantum yield is calculated using eq 1.[60]

$$\Phi_{unk} = \Phi_{std}\frac{(I_{unk}/A_{unk})}{(I_{std}/A_{std})}\left(\frac{\eta_{unk}}{\eta_{std}}\right)^2 \qquad (1)$$

where Φ_{unk} and Φ_{std} are the radiative quantum yields of the sample and the standard, I_{unk} and I_{std} are the integrated emission intensities of the corrected spectra for the sample and the standard, A_{unk} and A_{std} are the absorbances of the sample and the standard at the excitation wavelength (500 nm in all cases), and η_{unk} and η_{std} are the indices of refraction of the sample and the standard solutions, respectively. Excitation and emission slit widths were modified to adjust the luminescent intensity in a suitable range. All the spectroscopic measurements were performed at least in triplicate and averaged.

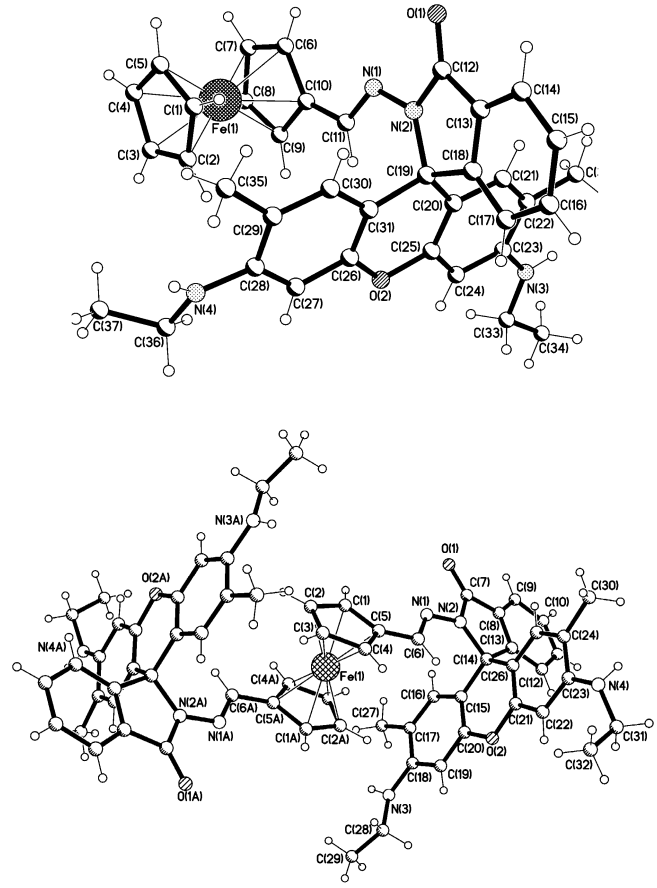

Figure 1. Molecular structures of **RF1** (top picture) and **RF2** (bottom picture) in spirolactam-ring tautomeric forms. Solvent molecules were omitted for clarity. Symmetry Code A: $-x + 1/2$, $-y + 1/2$, $-z$.

Results and Discussion

Structures of the Rhodamine-Ferrocene Chemosensors RFs. Rhodamine derivatives **RFs** were facilely synthesized from Rhodamine 6G by a two-step reaction (Scheme 1). The characteristic peak of the 10-carbon of **RFs** near 66 ppm in the ^{13}C NMR spectra suggests that the spirolactam form of **RFs** dominates in the solution (Supporting Information).[61,62] X-ray crystallography investigation (Figure 1) confirms the existence of the spirolactam form of **RF1** in the solid state. While the two aromatic planes of the Rhodamine moiety are almost perpendicular to each other with the dihedral angle of about 91°, the substituted Cp ring of the ferrocene moiety is almost coplanar with the attached phenyl ring, with the dihedral angle of 3.4° between the two planar fragments. Such a special spirolactam-ring tautomeric form of **RF1** inhibits the typical emission around 550 nm (excitation at 500 nm) of Rhodamine 6G within a relatively wide pH range.[63–65] Thus, it is expected that the emission

(58) *SMART and SAINT, Area Detector Control and Integration Software*; Siemens Analytical X-ray Systems, Inc.: Madison, WI, 1996.
(59) Sheldrick, G. M. *SHELXTL V5.1, Software Reference Manual*; Bruker, AXS, Inc.: Madison, WI, 1997.
(60) Fischer, M.; Georges, J. *Chem. Phys. Lett.* **1996**, *260*, 115–118; The fluorescence quantum yield was calculated by using Rhodamine 6G ($\Phi_f = 0.94$ in EtOH) as a reference.
(61) Anthoni, U.; Christophersen, C.; Nielsen, P.; Puschl, A.; Schaumburg, K. *Struct. Chem.* **1995**, *3*, 161–165.
(62) Zheng, H.; Qian, Z. H.; Xu, L.; Yuan, F. F.; Lan, L. D.; Xu, J. G. *Org. Lett.* **2006**, *8*, 859–861.
(63) Lee, M. H.; Wu, J. S.; Lee, J. W.; Jung, J. H.; Kim, J. S. *Org. Lett.* **2007**, *9*, 2501–2504.

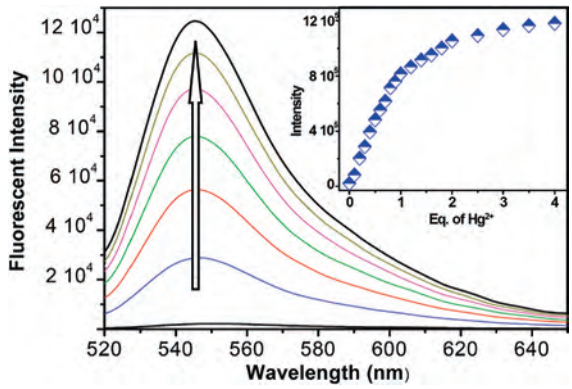

Figure 2. Fluorescent response of **RF1** (1 μM) upon addition of Hg^{2+} in an aqueous solution (0.1 M KNO_3), the inset picture shows the fluorescence titration profile around 550 nm at the excitation wavelength of 500 nm. Spectra were recorded every 4 min after adding Hg^{2+}.

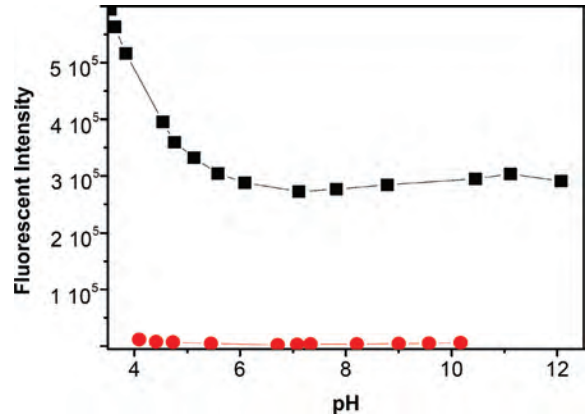

Figure 3. pH-Dependent fluorescence responses of **RF1** (10 μm, red circles) and **RF1** (10 μm) plus Hg^{2+} (20 μm, dark squares) in aqueous solution. The luminescence intensities were recorded at 550 nm with the excitation wavelength of 500 nm.

of **RF1** would be triggered and turned on when it was bound to the target cations. In addition, the coplanar configuration allows the conversion of the binding information into electrochemical signals through the electron delocalization within the ferrocene moiety and the phenyl ring of the rhodamine moiety.[66,67] Single crystal structural analysis of **RF2** also revealed that both the two rhodamine groups are present in the spirolactam form in the solid state. Two aromatic rings in one rhodamine moiety keep nearly perpendicular to each other with the dihedral angle about 93°. The spatial interactions between the two rhodamine groups cause the significant twist between the ferrocene moiety and the attached phenyl ring, with the dihedral angle between the two planar fragments of 22°.

Fluorescent Detection of Hg^{2+} in Water. An aqueous solution of **RF1** is selected for the spectral investigation. The free **RF1** solution, as expected, exhibits very weak fluorescence (excited at 500 nm) in neutral water. Upon addition of Hg^{2+}, the emission band at about 550 nm appears and develops (Figure 2). The emission band is reasonably assigned to the delocalized xanthene tautomer of the rhodamine group.[47,64] The similar emission profile to that of the free rhodamine suggests that the introduction of the ferrocenyl group does not compromise the typical emission of the rhodamine fluorophore.[68,69] The titration curve shows a steady and smooth increase until a plateau is reached with the quantum yield $\Phi = 0.38$ at the plateau (Figure 2). The Benesi−Hildebrand analysis of the emission data[70,71] gives a 1:1 stoichiometry for the **RF1**-Hg^{2+} complexation species, with an association constant (K_a) being calculated as 1.16 ($\pm$0.04) $\times$ 10^6 M^{-1}. The pH-controlled emission measurements (Figure 3) revealed that **RF1** can respond to Hg^{2+} in the pH range from 5.5 to 12.0 with the fluorescent intensity varying less than 10%, while the luminescence of the free **RF1** can be negligible. When the pH value is lower than 5.0, the fluorescence enhancement occurs also upon the coordination of Hg^{2+}, but the luminescence intensity of the free **RF1** increases slowly with the decreasing pH values. **RF1** facilitates quantification of the concentration of Hg^{2+} in aqueous solutions in a wide pH range.

Usually, a highly selective probe for Hg^{2+} that gives a positive response rather than fluorescent quenching upon analyst binding is preferred to promote the sensitivity factor. The fluorescence enhancement effects of various metal ions on **RF1** in water (10 μM) were investigated (excitation at 500 nm). As illustrated in Figure 4, no significant spectral changes of **RF1** were observed in the presence of alkali-, alkaline-earth metals, such as Na^+, K^+, Mg^{2+}, Ca^{2+} (1.25 mM) and the first-row transition metals Mn^{2+}, Fe^{2+}, Co^{2+}, Ni^{2+}, and Cu^{2+}(0.50 mM), respectively. Even the presence of 0.50 mM excess of Zn^{2+}, Cd^{2+}, as well as Pb^{2+} and Ag^+, could not bring any obvious fluorescence change. Furthermore, the competition experiments revealed that the Hg^{2+}-induced luminescence enhancement is unaffected in the presence millimolar quantities (1.25 mM) of environmentally relevant alkali-, alkaline-earth metals. In addition, the first-row transition metal ions including Mn^{2+}, Fe^{2+}, Co^{2+}, Ni^{2+}, and Cu^{2+}, as well as Pb^{2+} and Ag^+ (0.50 mM), do not interfere with the Hg^{2+}-induced fluorescence enhancement (the concentration of Hg^{2+} is 0.10 mM), confirming the remarkable selectivity of the probe **RF1** (10 μM) for Hg^{2+}.

Unlike most of other rhodamine- or fluorescein-based Hg^{2+} sensors, **RF1** does not show a diminished fluorescence turn-on following the Hg(II) binding in the neutral pH region without chloride ion.[72,73] Figure 5 shows the effects of anions on the fluorescence response **RF1** to Hg^{2+} in aqueous solutions. In the presence of KX (0.1M, X = OAc^-, F^-, Cl^-, Br^-, NO_3^-), only negligible fluorescence changes were

(64) Wu, J. S.; Hwang, I. C.; Kim, K.-S.; Kim, J. S. *Org. Lett.* **2007**, *9*, 907–910.
(65) Wu, D. Y.; Huang, W.; Duan, C. Y.; Lin, Z. H.; Meng, Q. J. *Inorg. Chem.* **2007**, *46*, 1538–1540.
(66) Yang, H.; Zhou, Z.; Huang, K.; Yu, M.; Li, F.; Yi, T.; Huang, C. *Org. Lett.* **2007**, *9*, 4729–4732.
(67) Plenio, H.; Yang, J.; Diodone, R.; Heinze, J. *Inorg. Chem.* **1994**, *33*, 4098–4104.
(68) Xiang, Y.; Tong, A. J. *Org. Lett.* **2006**, *8*, 1549–1552.
(69) Mao, J.; Wang, L.; Dou, W.; Tang, X.; Yan, Y.; Liu, W. *Org. Lett.* **2007**, *9*, 4567–4570.
(70) Kuntz, I. D.; Gasparro, F. P.; Johnston, M. D.; Taylor, R. P. *J. Am. Chem. Soc.* **1968**, *90*, 4778–4781.
(71) Lin, Z. H.; Xie, L. X.; Zhao, Y. G.; Duan, C. Y.; Qu, J. P. *Org. Biomol. Chem.* **2007**, *5*, 3535–3538.
(72) Nolan, E. M.; Lippard, S. J. *J. Mater. Chem.* **2005**, *15*, 2778–2783.
(73) Nolan, E. M.; Racine, M. E.; Lippard, S. J. *Inorg. Chem.* **2006**, *45*, 2741–2749.

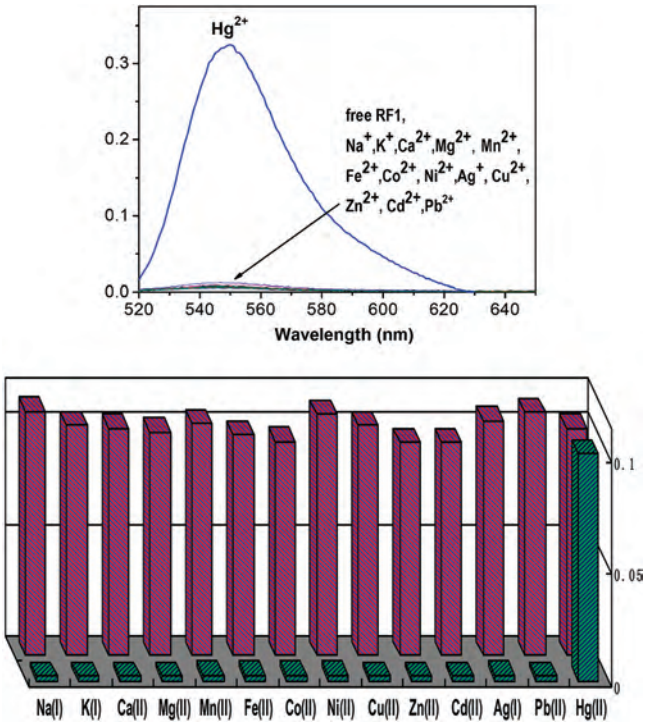

Figure 4. Top picture: Emission spectra of **RF1** (10 μM) in aqueous solution in the presence of 1.25 mM of Na^+, K^+, Ca^{2+}, and Mg^{2+}, 0.5 mM of the other cations, and 0.1 mM of Hg^{2+} at the excitation wavelength of 500 nm, respectively. Bottom picture: Fluorescence responses of **RF1** to various cations in an aqueous solution ([**RF1**] = 10 μM; λ_{ex} = 500 nm). The green bars represent the emission intensities of **RF1** in the presence of 1.25 mM of Na^+, K^+, Ca^{2+}, and Mg^{2+} and 0.5 mM of the other cations of interest, respectively. The violet bars represent the change of the emission that occurs upon the subsequent addition of 0.1 mM of Hg^{2+} to the above solution.

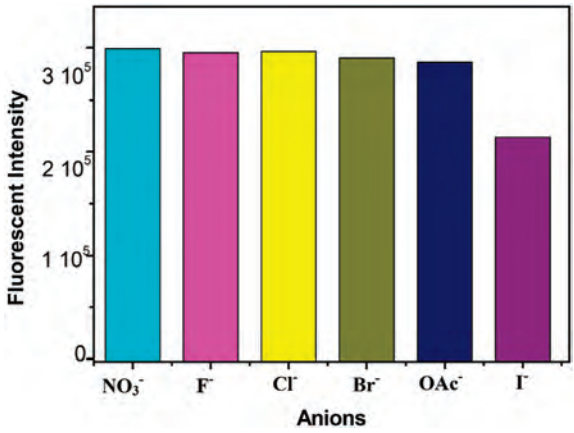

Figure 5. Effects of anions on the luminescence responses of **RF1** to Hg^{2+} in aqueous solutions. The bars exhibit the luminescence intensities of **RF1** (10 μM) upon the addition of Hg^{2+} (10 μM) in the presence of 100 μM of anions. Emission intensities were recorded at 550 nm with the excitation wavelength of 500 nm.

found in aqueous solution of **RF1** upon addition of Hg^{2+}. The presence of excess NaI could cause the disappearance of the color and decrease of fluorescence intensity of the titration solution, reflecting that the sensing could be a reversible process. Given that the presence of NaI has no effect on the emission profile of the free dye, the iodide-dependent fluorescence diminishment suggests the formation of a Hg^{2+}-I^- complexation, for example, HgI_4^{2-}.[48,62]

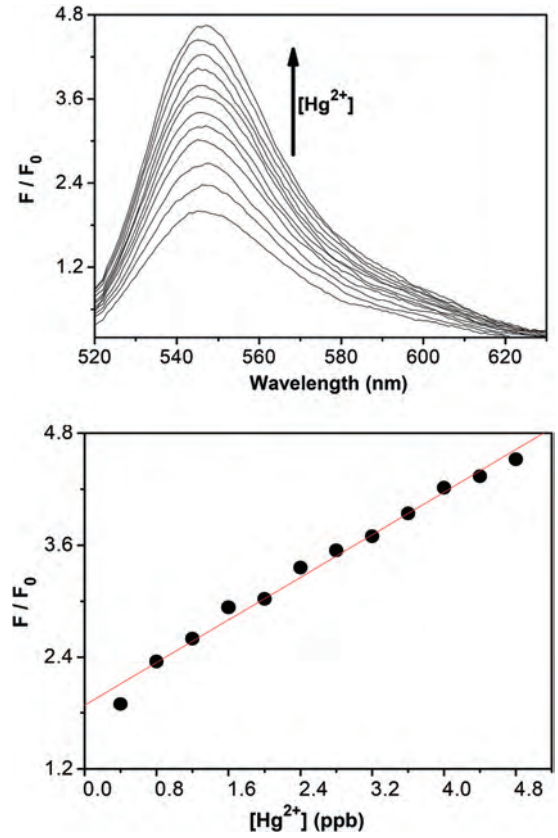

Figure 6. Top picture: Fluorescent response of **RF1** (0.1 μm) upon addition of Hg^{2+} by 0.4 ppb in an aqueous solution. Bottom picture: the fluorescence intensities at 550 nm. Excited at 500 nm, the emission intensities were recorded at 550 nm every 4 min after adding Hg^{2+}.

RF1 Performance in Natural Water Samples. Generally, the application of small molecular fluorescence detectors for Hg^{2+} in natural water samples presents a unique set of challenges, which requires detailed studies of sensor performance in the environmental milieu and method/device design. Owing to its optical Hg^{2+}-induced brightness, **RF1** is sensitive enough to detect environmentally relevant concentrations of Hg^{2+} ions in natural water. Addition of 2 ppb of Hg^{2+} ions (the maximum U.S. EPA limit for allowable levels of Hg^{2+} ions in drinking water)[34] to an aqueous solution of **RF1** affords a 3-fold increase of the emission intensity. The fluorescence profile of **RF1** (0.1 μM) upon the titration of Hg^{2+} is shown in Figure 6 and demonstrates that the limit of detection for Hg^{2+} is at the ppb level. Under the experimental conditions, the fluorescence intensities of the solution of **RF1** are nearly proportional to the amount of Hg^{2+} (0.4−5 ppb, $R^2 = 0.99$), indicating that **RF1** is capable of distinguishing between the safe and toxic levels of inorganic mercury in drinking water.

As an important step toward the objective of operating the sensor in natural water samples, we next tested the responding ability of **RF1** to Hg^{2+} in natural water. Samples were collected from two significantly different sources: the seawater from the Yellow Sea (Dalian), and the freshwater from the West Hill Reservoir (one of the water sources for Dalian). As shown in Figure 7, **RF1** shows ca. 3-fold fluorescence enhancement in samples spiked with 2 ppb of Hg^{2+} in each case. These results clearly show that **RF1** can

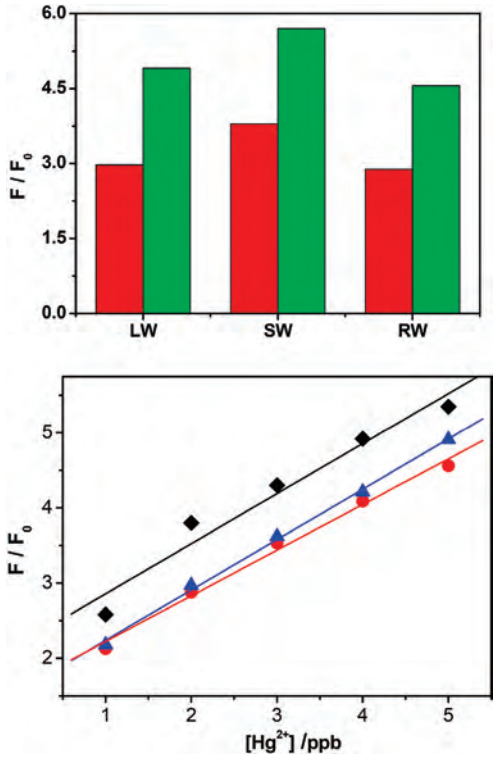

Figure 7. Top picture, respective response of 0.1 μM **RF1** to 2 ppb (red) and 5 ppb (green) of Hg^{2+} added to natural water samples: seawater (SW), reservoir fresh water (RW), and laboratory pure water (LW). Bottom picture, linear fluorescence response of **RF1** (0.1 μM) in natural water samples: seawater (black diamonds), reservoir water (red circles), and laboratory pure water (blue triangles) upon addition of Hg^{2+} by 1 ppb. The response (F) is normalized to the emission of the free sensor (F_0). The samples were excited at 500 nm, and the emission intensities were recorded at 550 nm every 4 min after adding Hg^{2+}.

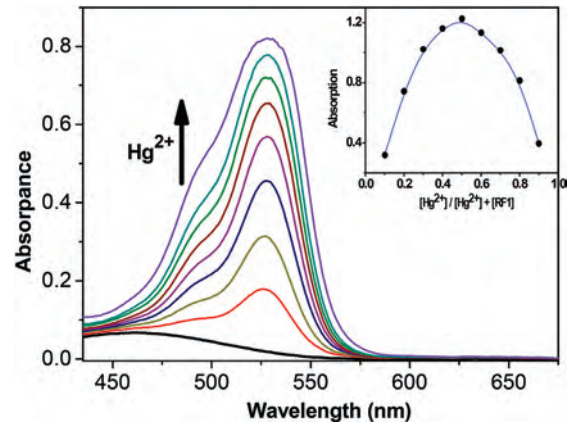

Figure 8. Absorption spectra of **RF1** (50 μM), upon addition of increasing amount of Hg^{2+} in aqueous solution. The inset shows the Job's plots evaluated from the absorption at 535 nm of **RF1** and Hg^{2+} with a total concentration of 125 μM in an aqueous media (CH_3CN/H_2O, 70:30, 100 mM KNO_3, T = 25 °C).

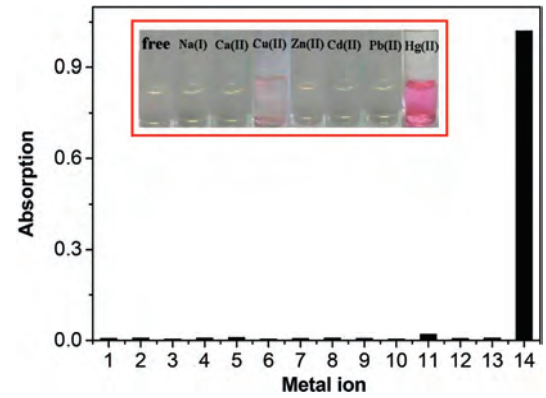

Figure 9. Absorption at 535 nm of **RF1** (50 μM) in an aqueous solution in the presence of 5 equiv of different metal ions. Horizontal axis key: 1, Na^+; 2, K^+; 3, Ca^{2+}; 4, Mg^{2+}; 5, Mn^{2+}; 6, Fe^{2+}; 7, Co^{2+}; 8, Ni^{2+}; 9, Ag^+; 10, Pb^{2+}; 11, Cu^{2+}; 12, Zn^{2+}; 13, Cd^{2+}; 14, Hg^{2+}. The inset exhibits the color changes of **RF1** (50 μm) after addition of 10 equiv of different metal ions.

detect Hg^{2+} in the solutions with a much more complicated composition relative to that of the laboratory buffer. Furthermore, under the experimental conditions, the fluorescence intensities of **RF1** in natural water samples are nearly proportional to the amount of Hg^{2+} (1−5 ppb), establishing that **RF1** is capable of distinguishing between the safe and the toxic levels of Hg^{2+} in the natural environment, which can reach the maximum China Standardization Administration (SA) limitation (1 ppb) for allowable levels of Hg^{2+} ions in drinking water.[74] Despite that there are several small molecular chemosensors that have the potential to detect Hg^{2+} in aqueous solutions at the ppb level,[36,37] **RF1** is the first one that can monitor Hg^{2+} below 1 ppb with the fluorescent responses still proportional to the amount of Hg^{2+} in natural water.

Naked-Eye Detection of Hg^{2+} in Aqueous Solution. The absorption spectrum (Figure 8) of **RF1** exhibited a weak band centered at ca. 460 nm (log ε = 3.08), which can be ascribed to the metal-to-ligand charge transfer of the ferrocenyl group.[22,75] Upon the addition of Hg^{2+}, the peak around 535 nm is significantly enhanced with log ε = 4.32, suggesting the formation of the ring-opened tautomer of **RF1** upon Hg^{2+} binding.[47,64] In this case, the titration solution exhibited an obvious and characteristic color change from colorless to pink (Figure 9). **RF1** thus can be used as a "naked-eye" detector of Hg^{2+} in aqueous solution. Quantitatively, the absorption of **RF1** at 535 nm increased linearly with the Hg^{2+} concentration. The lowest detectable threshold of 0.25 μM (50 ppb) meets the discharge limit for industrial wastewater according to the U.S. EPA standard[76] or the China SA standard.[77] In fact, the neutralized chlor-alkali electrolysis wastewater, one of the main anthropogenic sources of inorganic mercury,[78] has so high a mercury concentration, up to 3−10 mg/L, that the easy and cheap method of using a conventional spectrophotometer in standard conditions can be utilized to detect the concentration of mercury in the wastewater during the whole process from the factory to the wastewater treatment plants (WWTPs), ensuring safe discharge into the environment.

(74) Standardization Administration of the People's Republic of China, Standard examination methods for drinking water - Metal parameters, GB/T 5750.6- 2006.
(75) Janowska, I.; Miomandre, F.; Clavier, G.; Audebert, P.; Zakrzewski, J.; Thi, K. H.; Ledoux-Rak, I. *J. Phys. Chem. A* **2006**, *110*, 12971–12975.
(76) U.S. EPA *Regulatory Impact Analysis of the Clean Air Mercury Rule*; EPA-452/R-05−003; U.S. EPA: Research Triangle Park NC, 2005.
(77) Standardization Administration (SA) of the People's Republic of China, *Integrated wastewater discharge standard*, GB 8978- 1996.
(78) Dobler, I. W.; Canstein, H. V.; Li, Y.; Timmis, K. N.; Deckwer, W. D. *Environ. Sci. Technol.* **2000**, *34*, 4628–4634.

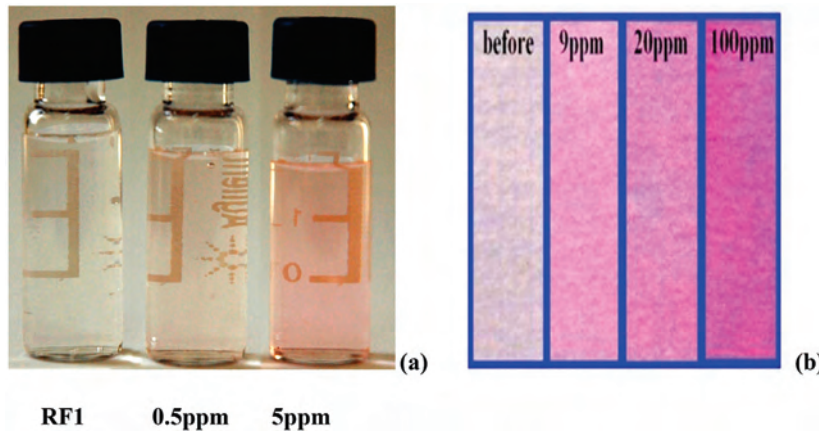

Figure 10. Color changes (a) of **RF1** (10 μM) in aqueous solutions in the presence of Hg^{2+} with concentrations of 0, 0.5, and 5 ppm. (b) Test papers having **RF1** before and after immersion in 9, 20, and 100 ppm Hg^{2+} in distilled water, respectively.

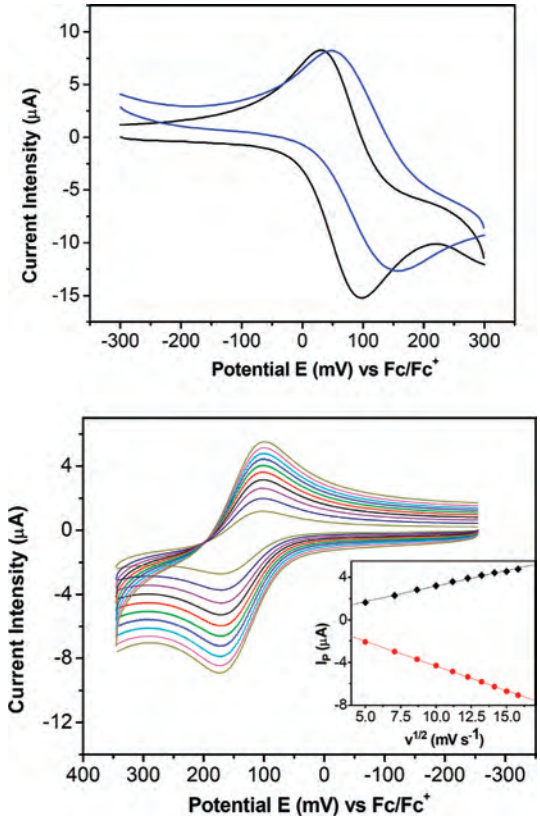

Figure 11. (top) CV in CH_3CN (5.0×10^{-4} M) of free **RF1** (black) and after formation of the **RF1**-Hg^{2+} complexation species (blue). (bottom) The family of CV curves of the **RF1**-Hg^{2+} complexation species showing the changes of current with the scan rate, $(n\text{-Bu})_4NClO_4$ (100 mM) as supporting electrolyte. The inset shows plots of anodic and cathodic peak currents versus the square root of the scan rates, $v^{1/2}$.

Figure 10a exhibits the color changes of aqueous solutions containing **RF1** (10 μM) in the absence and presence of Hg^{2+} in neutral aqueous solutions at the ppm level. Obviously, it is possible to detect Hg^{2+} at ppm levels in natural water by naked eye inspection. To further realize the practical application, the sensor **RF1** was prepared as a test paper to valuate its capability of selectively detecting Hg^{2+} in natural water. Figure 10b exhibits the color changes of the test papers before and after being immerged into Hg(II)-containing samples with different concentrations in natural water. It is possible with the in situ method to detect ppm level of Hg^{2+} in natural water by the naked eye inspection without any spectroscopic instruments. Although the detection limits of the naked eye inspection in natural water is not so low as the discharge limit for industrial wastewater (50 ppb), we anticipate that this procedure might be of interest as a promising route for the design of new and improved molecular sensors for the rapid colorimetric screening of Hg^{2+}. In fact, the work related to the development of cheap and effective new sensors for detecting toxic contaminations in the wild or undeveloped regions is underway in our laboratories.[79,80]

Meanwhile, no significant color change from colorless to pink is observed in the presence of some transition-metal ions, such as Mn^{2+}, Fe^{2+}, Co^{2+}, Ni^{2+}, and group 12 ions Zn^{2+} Cd^{2+}, as well as Pb^{2+} and Ag^{+}, even in a high concentration (i.e., mM level, Figure 9). Only the addition of Cu^{2+} into the solution of probe **RF1** (50 μM), under the same conditions, can induce the very small color change from colorless to pink. With further investigations, no plateau can be observed in the titration curve even when 3 mM solution of Cu^{2+} is added (Supporting Information, Figure S2); thus, the interference caused by the presence of Cu^{2+} is quite weak and could be negligible.[81] More interestingly, the fluorescent titrations of the aqueous solutions of **RF1** (1 μM) upon the addition of Hg^{2+} in the presence of selected heavy metal competing cations Cu^{2+}, Cd^{2+}, and Pb^{2+} (10 μM) showed that the association constants derived from the titration curves are almost identical (1.0×10^6 M^{-1}) with a little variation ($\leq$15%) compared to that of the free chemosensor **RF1** (Supporting Information, Figures S3−S5), strongly indicating the lack of interference of these competitive transition metal ions in the detection of Hg^{2+}. Hence, the highly sensitive and selective rhodamine-based probe for Hg^{2+} is water-

(79) Lin, Z. H.; Ou, S. J.; Duan, C. Y.; Zhang, B. G.; Bai, Z. P. *Chem Commun.* **2006**, 624–626.
(80) Needham, R. *Chem. Technol.* **2006**, *3*, T10.
(81) On the basis of the same simulation procedure, the UV−vis titration of **RF1** (50 μM) upon addition of Cu^{2+} demonstrates a 1:1 Cu^{2+}-binding complexation behavior. The calculated association constant (1.5×10^3 M^{-1}) is quite smaller than that of the Hg^{2+}-binding complexation species (1.2×10^6 M^{-1}), and the presence of excessive Cu^{2+} (50 equiv) do not compromise the Hg-induced optical responses (2.5 equiv of Hg^{2+}) of **RF1**.

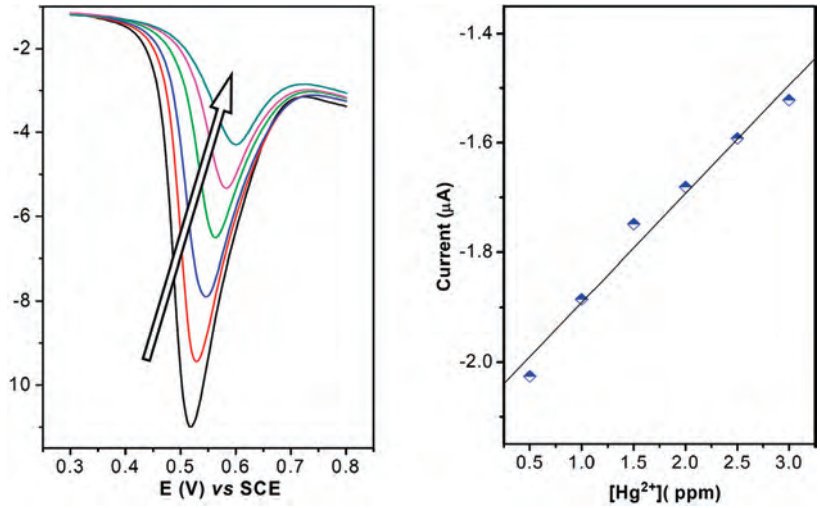

Figure 12. (left) DPV (50 ms pulse width) of free **RF1** (black) (5.0×10^{-4} M) upon the addition of Hg^{2+} at 1.0×10^{-4} M in CH_3CN/H_2O (70:30 v/v) showing the changes of peak potentials. (right) Plot of the currents of the oxidation peak in the CV (scan rate is 100 mV/s) of free **RF1** (5.0×10^{-4} M) upon the addition of Hg^{2+} at 0.5 ppm. $(n\text{-Bu})_4NClO_4$ (100 mM) was used as supporting electrolyte at 25 °C.

soluble and gives rise to a positive response upon binding, which might be of some practical utility.

Electrochemical Detection in Aqueous Media. Electrochemical methods, in particular, are extremely attractive from a practical standpoint because the signals can be easily read out on-site.[40,41,82] Because the ferrocenyl group is coplanar with the phenyl ring of the rhodamine moiety, the electronic density within the ferrocene group is influenced by the Hg^{2+}-binding induced electron portion of the optical sensitive rhodamine moiety. The "off-on" type chromogenical and fluorogenical responses corresponding to Hg^{2+}-binding induced conformational transformation from the spirolactam tautomer to the xanthene tautomer should be accompanied with a significant shift of the redox potential of the ferrocenyl group. As shown in Figure 11a, the cyclic voltammetry (CV) study of the substance **RF1** in an acetonitrile solution exhibits a reversible one-electron redox process around 65 mV vs Fc^+/Fc. Whereas no perturbation of the CV and the DPV is observed upon the addition of alkali or earth alkali metal ions, or Ni^{2+}, Zn^{2+}, Cd^{2+}, and Pb^{2+} metal ions,[83] the addition of 1 equiv Hg^{2+} could induce a significant anodical shift of the ferrocene/ferrocenium redox couple with $\Delta E_{1/2}$ of 50 mV and the appearance of a new peak at about −0.335 mV (Fc^+/Fc), which is assigned to the redox process of the Hg^{2+} in the **RF1**-Hg^{2+} complexation species.[66] The reversibility of the ferrocene/ferrocenium redox couple of **RF1** in the presence of 1 equiv Hg^{2+} is confirmed by the linear relation between peak currents and the square root of the scan rates, (inset in Figure 11) the small difference between anodic and cathodic peak currents, as well as the small peak-to-peak potential separations.

The selective redox response toward Hg^{2+} is also preserved even in the presence of water. The DPV measurements show an anodical shift ($\Delta E_{1/2} = 30$ mV) upon the complexation of Hg^{2+} in aqueous CH_3CN solution (CH_3CN/H_2O, 70:30) (Figure 12). A linear correlation between the redox potential shift and the concentrations of Hg^{2+} allows for a facile quantification. Furthermore, the linear correlation between the peak currents and the concentrations of Hg^{2+} in the cyclic voltammeter allows the quantitative analysis of Hg^{2+} at ppm levels with the limits of detection being 0.5 ppm.

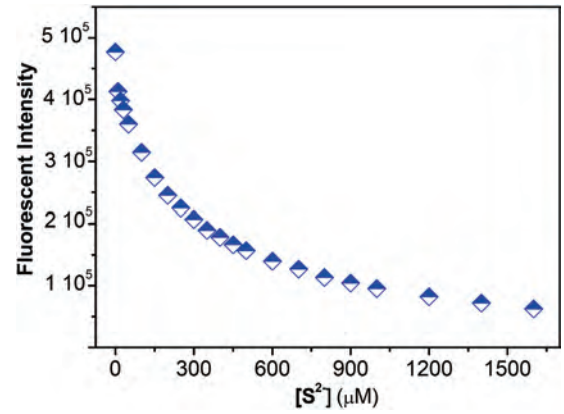

Figure 13. Fluorescence titration profile of the **RF1**-Hg^{2+} complexation species in an aqueous solution (10 μM) upon the addition of Na_2S. The intensities were recorded at 550 nm with the excitation wavelength of 500 nm. Spectra were recorded every 15 min after adding Na_2S.

Mechanism Studies of RF1-Hg^{2+} Complexation. The rhodamine framework is an ideal model from which to construct OFF-ON fluorescent chemosensors because of its particular structural property. As it is well-known, rhodamine derivatives with spirolactam structure are nonfluorescent, whereas ring opening of the spirolactam gives rise to a strong fluorescence emission. Without cations, these probes exist in a spirocyclic form, which is colorless and nonfluorescent. Addition of metal cation leads to a spirocycle opening via coordination[62,63,65,84–89] or irreversible chemical reaction,[47,48,64,90,91] resulting in the appearance of pink color and orange fluorescence. The addition of an aqueous solution of Na_2S (0.1M)[92,93] to the solutions of **RF1**-Hg^{2+} species diminished the fluorescence significantly with a smooth decreasing trace versus the concentrations of Na_2S that finally drops down to about 8% of the initial value (Figure 13).

(82) Crouse, M. M.; Miller, A. E.; Crouse, D. T.; Ikram, A. A. *J. Electrochem. Soc.* **2005**, *152*, D167−D172.
(83) The metal ions that exhibit obvious redox potential within this range, such as Cu^{2+}, Fe^{2+}, and Mn^{2+} were not checked.

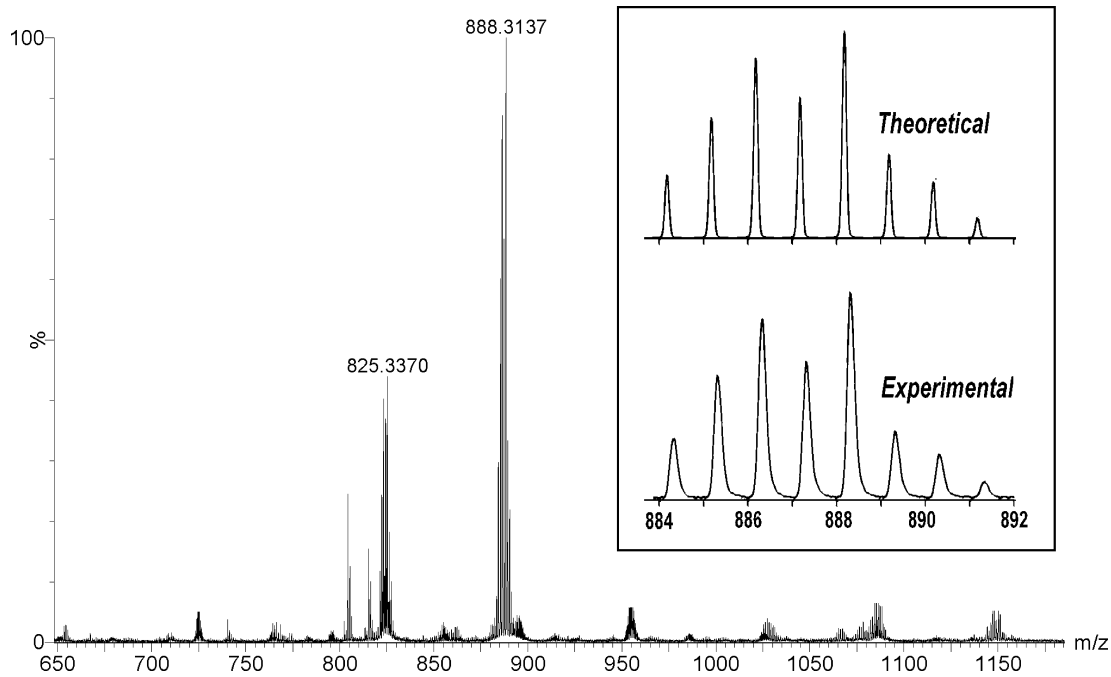

Figure 14. ESI-MS of the titration solution of **RF1** upon the addition of Hg^{2+}. The two main peaks at *m*/*z* of about 825.33 and 888.31 correspond to $[Hg(\mathbf{RF1})]^+$ and $[Hg(\mathbf{RF1})(NO_3)]^+$, respectively. The inset exhibits the calculated (top picture) and observed (bottom picture) isotopic patterns for the $[Hg(\mathbf{RF1})(NO_3)]^+$ cation.

Scheme 2. Proposed Binding Mode of **RF1** with Hg^{2+}[a]

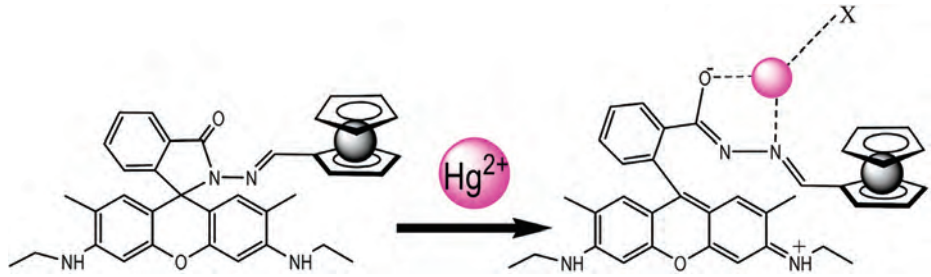

[a] **X** is the coordinating anion or solvent.

This is not surprising since S^{2-} has a reported K_d value of 10^{-50} M^2 for Hg^{2+} at a standard condition in the form of $[HgS_2]^{2-}$. Thus, the response of **RF1** to Hg^{2+} is reversible rather than a cation-catalyzed reaction.[94]

Job's plot evaluated from the absorption spectra of the titration solution (inset of Figure 8) exhibited the inflection point at 0.5, indicating the formation of a 1:1 **RF1**-Hg(II) coordination species in the aqueous solution. This 1:1 stoichiometry for the **RF1**-Hg^{2+} coordination species is further confirmed by the ESI-MS of the titration solution (Figure 14), which shows two peaks with *m*/*z* = 825.3 and 888.3, corresponding to the species $[\mathbf{RF1}\text{-Hg}]^+$ (m/z_{calcd} = 825.2) and $[\mathbf{RF1}\text{-Hg}(NO_3)]^+$ (m/z_{calcd} = 888.2), respectively. The presence of $[\mathbf{RF1}\text{-Hg}]^+$ found in the ESI-MS spectrum suggests that the deprotonation form of the **RF1** can be captured in the spectral conditions. The elemental analyses of the pure **RF1**-Hg^{2+} complex isolated also support the 1:1 stoichiometry for **RF1**-Hg complexation. The proposed binding mechanism of Hg^{2+} with **RF1** is shown in Scheme 2. Both the carbonyl O and the imino nitrogen atom together with Hg^{2+} involved in the binding event form a stable five-membered metallocycle that results in the opening of the spiro ring of **RF1** to establish the delocalized xanthene moiety, and the other coordination sites of Hg^{2+} may be completed by solvents and/or the counteranions. ^1H NMR experiments confirm the Hg^{2+}-binding ring opening mech-

(84) Kwon, J. Y.; Jang, Y. J.; Lee, Y. J.; Kim, K. M.; Seo, M. S.; Nam, W.; Yoon, J. *J. Am. Chem. Soc.* **2005**, *127*, 10107–10111.
(85) Xiang, Y.; Tong, A.-J.; Jin, P.-Y.; Ju, Y. *Org. Lett.* **2006**, *8*, 2863–2866.
(86) Zhang, X.; Shiraishi, Y.; Hirai, T. *Org. Lett.* **2007**, *9*, 5039–5042.
(87) Lee, M. H.; Kim, J. K.; Yoon, S.; Park, N.; Kim, J. S. *Org. Lett.* **2008**, *10*, 213–216.
(88) Soh, J. H.; Swamy, K. M. K.; Kim, S. K.; Kim, S.; Lee, S.-H.; Yoon, J. *Tetrahedron Lett.* **2007**, *48*, 5966–5969.
(89) Zhang, M.; Gao, Y.-H.; Li, M.-Y.; Yu, M.-X.; Li, F.-Y.; Li, L.; Zhu, M.-W.; Zhang, J.-P.; Yi, T.; Huang, C.-H. *Tetrahedron Lett.* **2007**, *48*, 3709–3712.
(90) Dujols, V.; Ford, F.; Czarnik, A. W. *J. Am. Chem. Soc.* **1997**, *119*, 7386–7387.
(91) Shi, W.; Ma, H. *Chem. Commun.* **2008**, 1856–1858.
(92) Findlay, D. M.; McLean, R. A. N. *Environ. Sci. Technol.* **1981**, *15*, 1388–1390.
(93) Armstrong, R. D.; Porter, D. F.; Thirsk, H. R. *J. Phys. Chem.* **1968**, *72*, 2300–2306.
(94) When titrating the isolated **RF1**-Hg^{2+} species upon addition of an aqueous solution of Na_2S, the spectra has to be recorded every 20 min after adding Hg^{2+} to make the reaction balance.

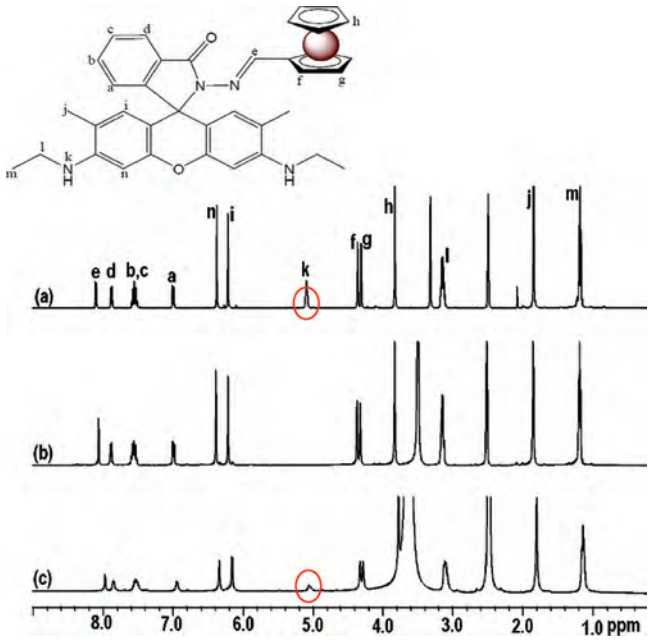

Figure 15. ^{1}H NMR data of (a) **RF1** (1 mM, in DMSO-d_6), **RF1**-Hg^{2+} complexation species (1 mM, in DMSO-d_6) in the absence (b) and in the presence (c) of 10 equiv Na_2S in D_2O solution.

anism. As shown in Figure 15, the ^{1}H NMR spectrum of free **RF1** exhibits a chemical shift of *NH* at about 5.30 ppm,[65] whereas this typical chemical shift is absent in the NMR spectrum of the **RF1**-Hg^{2+} complex. This absence of the chemical shift of NH suggests that these NH protons exhibit strong acidity and tend to leave in the solution, which might be an indicator of the formation of a delocalized xanthene tautomer of the rhodamine group upon the coordination of Hg^{2+}. The ^{1}H NMR spectrum thus might explain that the binding interaction between hydrazone and Hg^{2+} ion would result in the ring-opening of the spirolactam in **RF1**, which is responsible for the dual signal changes (color and fluorescence). The recovery of the chemical shifts of almost all protons in the free **RF1** upon the addition of Na_2S (Figure 15c) provides further proof of the reversibility in the **RF1**-Hg^{2+} complexation process.

The absence of the 1:2 stoichiometry for the **RF1**-Hg binding mode is probably due to the space effect of the large rhodamine unit and ferrocene units in **RF1.** It should be noted that such a special binding mode provides high selectivity toward Hg^{2+} over other metal ions. As shown in Scheme 3, the rhodamine derivatives with diethylenetriamine (**RH1**)[69] showed a higher affinity to Fe^{3+} with larger ionic radii than that of Cr^{3+}, whereas the more flexible triethylenetetriamine group in **RH2** displayed the opposite outcome as the affinity to Cr^{3+} with smaller ionic radii is stronger than that to Fe^{3+}. Meanwhile, the rhodamine B hydrazide[90] (**RH3**) was an irreversible chemodosimeter for selective detection of Cu^{2+} with larger ionic radii than those of Fe^{3+} and Cr^{3+} by opening the spiro-ring upon metal ion binding at the N, O atom positions, whereas the analogue compound **RH4**[85] displayed little response to Cu^{2+} as revealed in either the absorption or the ESI-MS spectra. Most importantly, acetylferrocene-rhodamine B hydrazide (**RF3**)[66] with the tiny alternation of the uncoordinated groups from ferrocenylmethylidene (**RF1**)

Scheme 3. Chemical Structures of Some Rhodamine-Based Chemosensors for Metal Cations

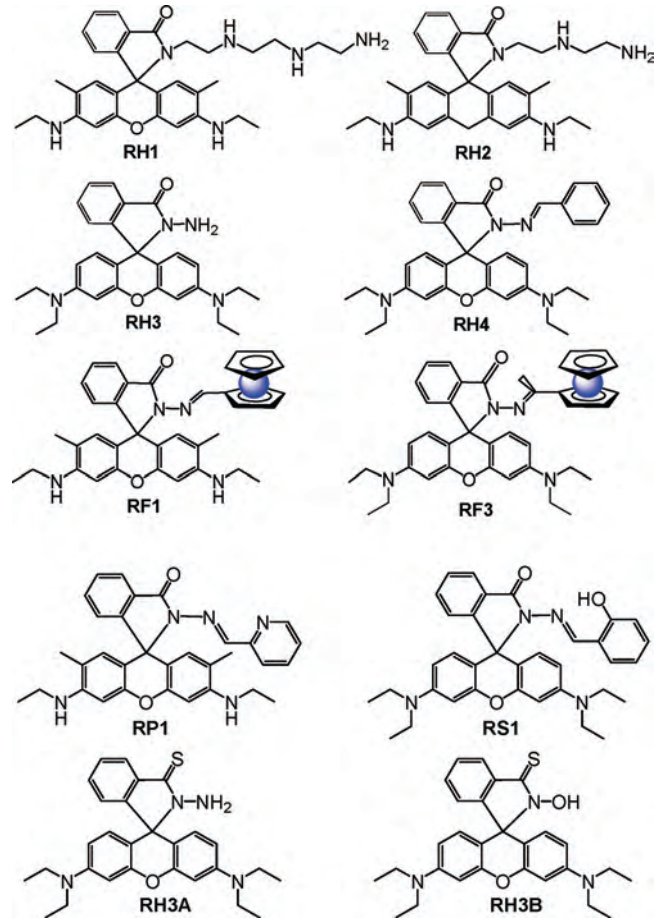

to ferrocenylethylidene (**RF3**) is insensitive to Hg^{2+} in the reported environment. It is reasonable to say that the spatial effect of large rhodamine unit and the ferrocene groups probably affects the binding ability to the first-row transition metals with constraint geometries and certain coordination numbers. Consequently, the lack of additional binding sites of **RF1** would make the probe show none or little coordination to any other metal ions but allow the most preferred mercuric ion to bind. To get insight into the roles that the spatial effect plays in sensing Hg^{2+}, ferrocene-rhodamine derivative **RF2**, which contains one ferrocene group and two rhodamine 6G moieties was used for spectral testing. Upon the addition of Hg^{2+} ion, **RF2** gave rise to considerable but smaller absorption and fluorescent spectral changes compared to those of **RF1**. In fact, as shown in Figure 16, in the presence of 5 ppb of Hg^{2+} ion, the fluorescent intensity of the aqueous solution of **RF1** (0.1 μM) exhibited about 2.5 times larger changes than those of **RF2** despite that **RF2** has two fluorescent active rhodamine groups. From the titration experiments, the association constant of **RF2** with the Hg^{2+} ion in aqueous solution was calculated as $2.8 \pm 0.2 \times 10^5$ M^{-1} on the basis of 2:2 stoichiometry (Figure 17), which can reflect the superior binding ability of **RF1** toward Hg^{2+} than that of **RF2** and further suggests that the spatial effect is one of the most significant contributors to the Hg(II) special binding. In addition, the Hg^{2+} binding to

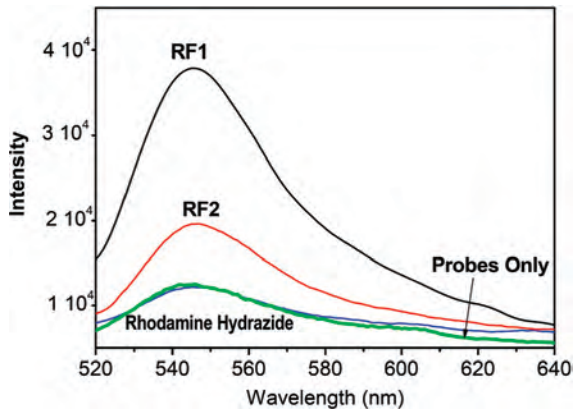

Figure 16. Fluorescence spectra of **RF1**, **RF2**, and Rhodamine 6G hydrazide (0.1 μm) upon the addition of Hg^{2+} (5 ppb) in aqueous solutions at the excitation wavelength of 500 nm.

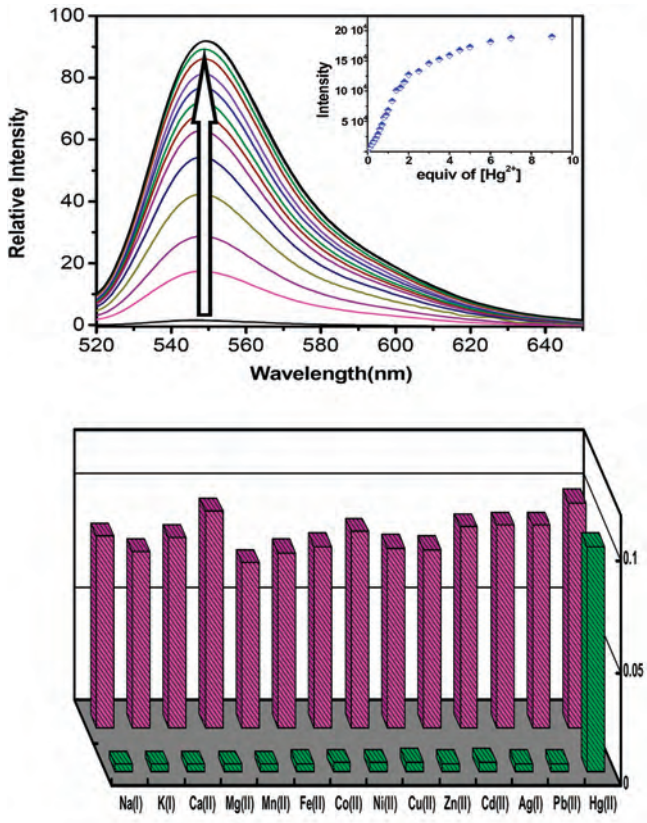

Figure 17. Top picture **:** Fluorescent response of 1 μM **RF2** upon addition of Hg^{2+} in an aqueous solution (0.1 M KNO_3). The inset shows the titration profile upon addition of the Hg^{2+} aqueous solution. Spectrum is recorded every 4 min after adding Hg^{2+}. Bottom picture: Fluorescence responses of **RF2** to various cations in an aqueous solution ([**RF2**] = 10 μM;). The green bars represent the emission intensities of **RF2** in the presence of 1.25 mM of Na^+, K^+, Ca^{2+}, and Mg^{2+} and 0.5 mM of the other cations of interest. The violet bars represent the change of the emission that occurs upon the subsequent addition of 0.1 mM of Hg^{2+} to the above titration solution. The emission intensities were recorded at 550 nm at the excitation wavelength of 500 nm.

RF2 cannot cause any significant potential shift of the ferrocene/ferrocenium redox couple.

Furthermore, the nitrogen-affinity characteristic of the Hg^{2+} ion is also an important factor for the designed **RF1** probe, which exhibits high selectivity for Hg^{2+} over other metal cations. As shown in Scheme 3, the pyridine-containing chemosensor **RP1** affords Hg^{2+}-specific fluorescence enhancement and shows a detection limit as low as a 2 ppb level in a DMF aqueous solution[65] The potential tridentate N_2O chelating capability leads to a poor selectivity toward Hg^{2+} over Cu^{2+}, whereas the presence of the phenol group allows the **RS1** probe[85] to exhibit Cu^{2+}-specific absorbance and fluorescence responses, and exhibits a good selectivity for Cu^{2+} over Hg^{2+}. The absorbance of **RH3A** exhibits significant responses toward Hg^{2+}, but **RH3B** does not under the same conditions, which suggests that the presence of a N atom rather than an O atom in the coordination environment benefits the selectivity toward Hg^{2+} over other metal ions. Hence, it is concluded that the unique selectivity for Hg^{2+} ion is partly due to several cooperative factors, such as the suitable coordination conformation of the Schiff-based receptor, the spatial effects of the uncoordinated ferrocenyl group, the large radius of the Hg^{2+} ion, and the nitrogen-affinity characteristic of the Hg^{2+} ion. It is possible that the low solvation energy of Hg^{2+} versus the other harder cations is also a contributing factor.

In summary, we have demonstrated that the incorporation of a ferrocenyl unit into a fluorescent moiety rhodamine-6G leads to an excellent Hg^{2+} sensing behavior in both electrochemical and optical detections. **RF1** can selectively bind Hg^{2+} over other Group 12 metals, most divalent first-row transition metals, and millimolar concentrations of various alkali and alkaline earth metals. The ppb level fluorescent detection limit coupled with the naked eye inspection for Hg^{2+} in natural water suggests the possibility of practical applications in toxicology and environment sciences. The preliminary investigations in natural water samples including seawater and freshwater indicate that **RF1** offers direct and immediate Hg^{2+} detection in complex media, pointing out its potential utility in the field. Our future research efforts will concentrate on the development of new testing methods to improve the recognition ability of **RF1** and its derivatives toward different ions in the practical environment and media.[95,96]

Acknowledgment. This work is supported by the National Natural Science Foundation and the Start-Up Fundation of Dalian University of Technology. The authors also thank the anonymous reviewers for helpful suggestions, and some of their opinions are directly used in the text, Ms. Liu for the assistance with the NMR measurements.

Supporting Information Available: X-ray structural data of **RF1** and **RF2** in CIF format, ^{13}C NMR spectra of **RF1** and **RF2**, additional spectroscopic data, and fitting procedure of the association constant (PDF). This material is available free of charge via the Internet at http://pubs.acs.org.

IC8004344

(95) Schmittel, M.; Lin, H. W. *Angew. Chem., Int. Ed.* **2007**, *46*, 893–896.
(96) de Silva, A. P. *Nature* **2007**, *445*, 718–719.